LLNL-PROC-750272

Enhanced exoplanet biosignature detection from an interferometer addition to low resolution spectrographs

David J. Erskine[a], Philip S. Muirhead[b], Andrew M. Vanderburg[c], and Andrew Szentgyorgyi[d]

[a]Lawrence Livermore Nat. Lab., Livermore, CA 94550
[b]Astronomy Dept., Boston University, Boston, MA 02215
[c]University of Texas, Austin, TX 78712
[d]Harvard-Smithsonian Center for Astrophysics, 60 Garden St, Cambridge, MA 02138

ABSTRACT

The physics of molecular vibration causes absorption spectra of atmospheric molecules to be a group of approximately periodic fine lines. This is fortuitous for detecting exoplanet biosignificant molecules, since it approximately matches the periodic sinusoidal transmission of an interferometer. The series addition of a 0.6 cm interferometer with a dispersive spectrograph creates moire patterns. These enhance detection by several orders of magnitude for initially low resolution spectrographs. We simulate the Gemini Planet Imager integral field spectrograph observing a telluric spectrum of native resolutions 40 and 70 for 1.65 and 2 micron bands– too low to resolve the fine lines. The interferometer addition increases the detectability of the molecular signal, relative to photon noise, to a level similar to a R=4400 (at 1.65 micron) or R=3900 (at 2 micron) spectrograph.

Keywords: High resolution spectroscopy, Externally Dispersed Interferometry, Resolution Boosting, Fourier Transform Spectroscopy, Exoplanets, Atmosphere, Molecules, Biosignature

1. INTRODUCTION

Having both spatial and spectral resolution is desirable in a scientific instrument, but engineering tradeoffs usually diminish having both simultaneously in large amounts. For example, Figure 1 shows a detector section from the Gemini Planet Imager integral field spectrograph[1](IFS), where a lenslet array and prism creates an array of spectra describing different regions of the image. The number of pixels available for each spectra is severely limited due to proximity of neighboring spectra, limiting the spectral resolution.

Author information:
D.E.: erskine1@llnl.gov

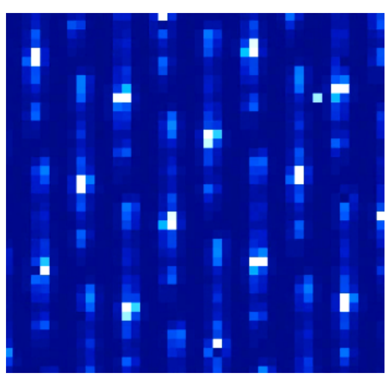

Figure 1. Example section of Gemini Planet Imager integral field spectrograph[1] showing many close packed spectra, one for each spatial location of a target image. The number of pixels available, and hence spectral resolution, is severely limited by the proximity of neighboring spectra.

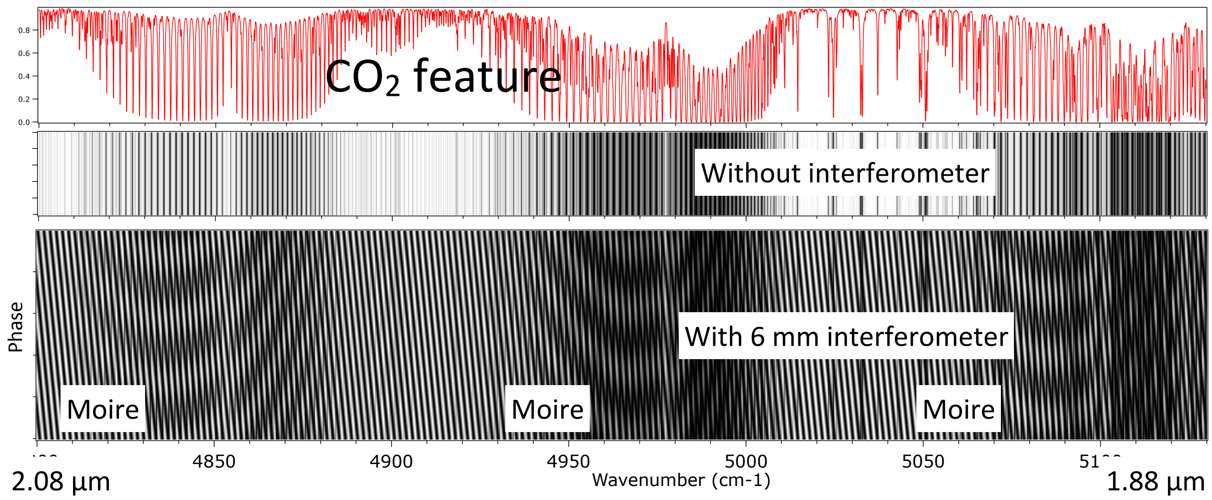

Figure 2. (Top) Portion of near infrared telluric spectrum (intensity vs wavenumber) 4800-5130 cm^{-1} having three prominent CO_2 features. (Middle) Same spectrum where intensity is represented by grayscale, and Y-axis has no meaning. (Bottom) Telluric spectrum is multiplied by a 5.8 mm delay sinusoidal interferometer transmission spectrum. The interferometer phase (which is increment in delay relative to wavelength) is splayed linearly along the Y-axis to reveal moiré patterns. Note the three "smile" like moire features corresponding to the three CO_2 features. These are high frequency information beaten down to low frequencies which can better survive a low resolution spectrograph. Data is taken by measuring at least two or three phase stepped spectra at 180 or 120 degrees of interval, to separate fringing from nonfringing components.

2. METHOD: EXTERNALLY DISPERSED INTERFEROMETRY

We introduce externally dispersed interferometry (EDI) as a solution to increasing the resolution of any spectrograph, and an IFS in particular. This technology has been demonstrated on other linear and echelle spectrographs in the visible and near infrared,[2–6] to boost the spectral resolution by a factor of two to an order of magnitude, by placing an interferometer in series with the beam and taking multiple exposures while stepping the interferometer delay. Each exposure is processed separately, and then a composite signal formed. The latter has a higher effective resolution than the spectrograph used alone, limited only by the highest delay of a contiguous range of delays used. Doppler velocities have also been measured by EDI[6–10] and a new exoplanet found.[11]

2.1 Incomplete delay coverage proposed

In our prior reports we described EDI using delays that contiguously covered a range of delay space, without significant gaps. This has the advantage of producing an accurate shape of the spectrum, because all frequencies along the dispersion axis (features per wavenumber) are sensed. (The frequency being sensed is proportional to the interferometer delay.)

However, for economic use of photons in measuring the amount of a known spectral signature, a single or small number of delays can be used that do not contiguously fill delay space. This is appropriate when the shape of the feature, such as due to molecular absorption in an atmosphere, is known. This scheme allows detection of the molecule at a much higher effective resolution, since precious exposure time is not wasted on delays having lower information content. The optimal delay region is near a maximum in the Fourier transform of the spectral feature.

An incomplete delay coverage has been used previously in EDI for measurement of Doppler radial velocities,[7–11] so the EDI data taking method at an observatory setting is well demonstrated.

3. APPLICATION: MEASURING CO_2 PRESENCE IN SPECTRA

Exoplanet atmospheric molecules (water, CO_2, methane etc) vibrational spectra normally require high resolution to detect, much higher than what the example IFS can resolve. But fortuitously, because the physics of vibrating

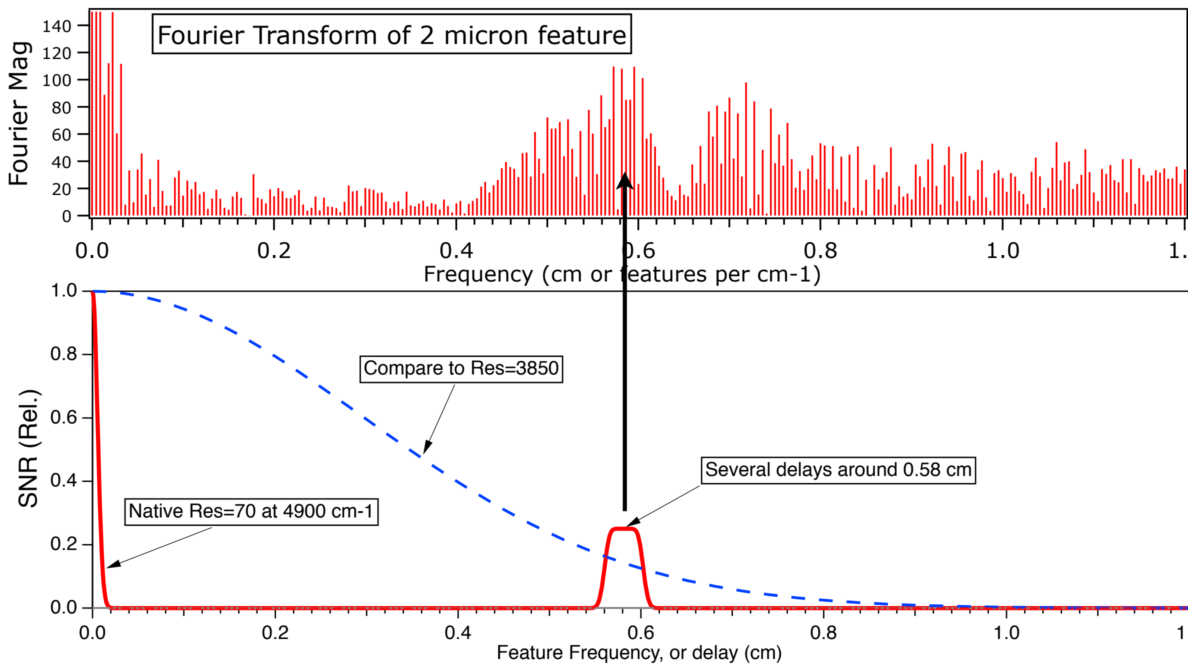

Figure 3. (Top) Fourier Transform of a section of the CO_2 feature near 2 μm (4800-5100 cm^{-1}) showing concentration of energy above 0.4 cm and a local peak near 0.6 cm. (Bottom) Red curve is filtering behavior, instrument response, or modulation transfer function (MTF) of proposed EDI when a small set of delays is used to cover a region around 0.58 cm, and the native resolution is R=70. A single delay would produce a peak of same width as the native (at the origin) and of height 0.5. Using multiple delays spreads the area under the peak following a quadrature or root mean square sum rule where area under square of function is same as a single delay, assuming the same exposure time is redistributed among several delays. The dashed blue curve is the response of a classical spectrograph of R=3850, for comparison. Vertical axis plots signal relative to same continuum photon noise, scaled such that both R=70 and R=3850 classical spectrograph cases have the same size pixels, and thus same noise in limit of broad features (zero feature frequency or delay). Horizontal axis is feature frequency or interferometer delay, which both have units of cm.

molecules create a quasi-periodic set of 30-40 absorption lines as a fingerprint (Figure 2, top), they are remarkably easier to detect with a small interferometer insert to the spectrograph beampath.

By overlaying a periodic grid with the high resolution spectrum, Figure 2 bottom shows how a small (6mm) EDI interferometer, which produces a periodic transmission with similar spacing as these molecular lines, creates extremely strong moire patterns for this fingerprint. The goal of the measurement is to detect these moire patterns. The amount of molecular spectral feature is proportional to the magnitude of the moire component relative to the ordinary signal.

Figure 3 bottom, shows that this moire signal for the 2 micron band is detected having a photon limited sensitivity similar to a R$\sim$4000 spectrograph, as indicated by the similar height of the red EDI peak to the dashed blue curve, where the latter represents a classic spectrograph of 3850 resolution. (A similar calculation for the feature in the 1.6 micron band yields an effective resolution of near 4400.)

Figure 3 top, shows that the Fourier transform of the 2 μm CO_2 feature has a peak in the 0.5 to 0.6 cm range, and a dearth of energy from 0.05 to 0.4 cm. (Frequency and delay have the same units of cm here). Thus to economize on use of photons for the detection of CO_2, one should place the sensitivity of EDI (set by its interferometer delay) at this maximum. Conversely, there is little information in the 0.05 to 0.4 cm range. If the goal was to measure a shape of an unknown spectrum, then probing a contiguous range of delays over a wide extent would be necessary. However, here we already know the expected shape of the CO_2 contribution, apart from a Doppler shift.

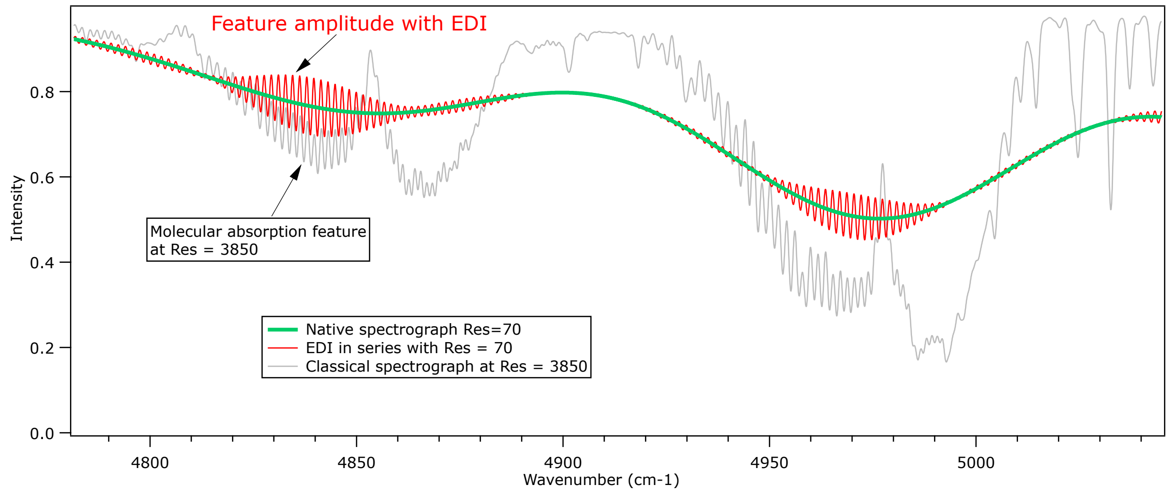

Figure 4. Simulated measurement of the telluric spectrum using three calculated instrument responses to produce three curves: native R=70 (green), classical R=3850 (gray), and EDI (red). The different MTF of the bottom pane of Fig. 3 are multiplied against its top pane, then inverse Fourier transformed to wavenumber space. We use the localized native peak at 0 cm, the entire blue dashed curve, and the localized EDI peak at 0.58 cm to produce the green, gray and red results here. The R=3850 classical case (gray) resolves some of the fine lines enough for detection of this feature. However, the R=70 native (green) cannot. The EDI peak at 0.58 cm produces the red curve, which produces a similar amplitude of fine lines of the CO_2 feature as the gray curve for some portions of the spectrum. This is noteworthy because the EDI boosts the low R=70 resolution to effectively higher resolution to make a measurement otherwise not possible for this device.

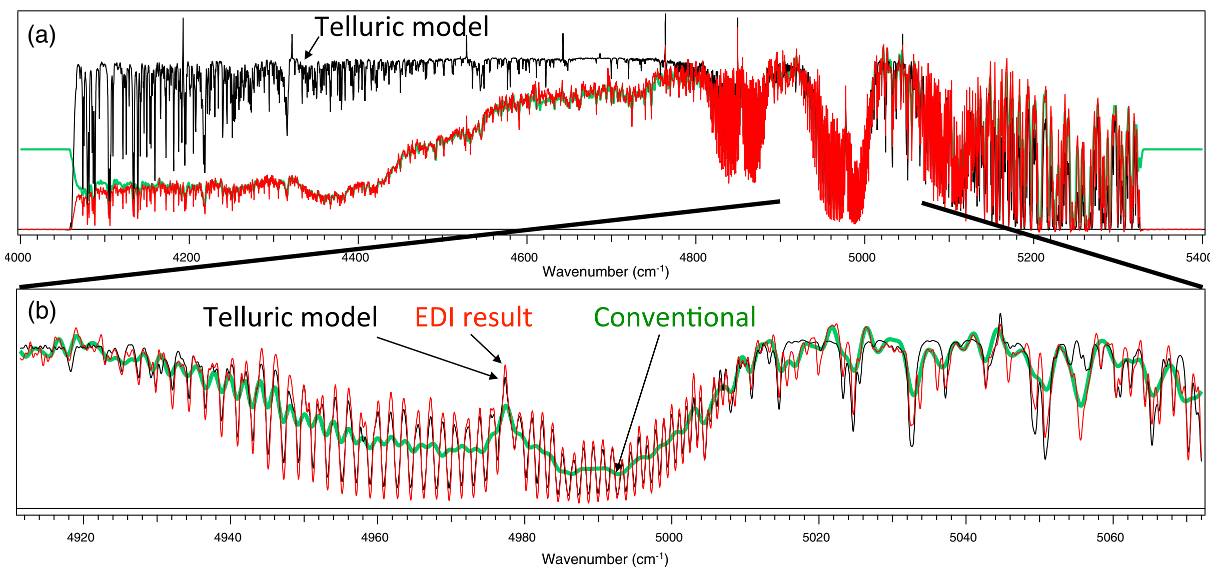

Figure 5. Experimental demonstration measuring CO_2 features near 5000 cm^{-1} in telluric spectrum of HD219134 using T-EDI at Mt. Palomar Hale telescope. The native 2700 resolution TripleSpec NIR disperser was boosted 4x to 11000 by several contiguous delays up to 2 cm. In contrast, the proposal today is to economize this measurement by using only the delays near 0.6 cm, since the CO_2 feature shape is already known. Also, a lower resolution (70 instead of 2700) native disperser would be used. Black is telluric model, red is T-EDI result, green is conventional disperser alone. The red and green curves are below the black curve at low wavenumber side because of disperser coloration. Reproduced from Fig. 24 of Ref. 2.

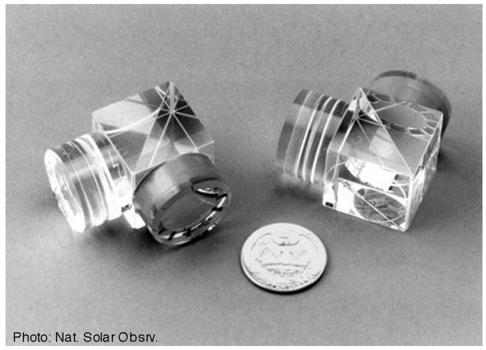

Figure 6. Example of compact and monolithic fixed delay interferometers which could be used for EDI. These were made by the National Solar Observatory for measuring Doppler shift of sunlight. Changing a voltage to a PZT transducer upon which one of the mirrors is mounted can dither the delay by the required amount, about a wavelength. Rather than the our prior strategy of using one interferometer apparatus with a filter wheel holding different etalons to swap in to produce different delays, another possible strategy is to mount different whole interferometers mounted in the filter wheel, inserting them in sequence into the beam.

A single delay could in principle be used, but we find that there is some advantage in using multiple exposures to spread the range of delays used slightly to a small range, such as the $\sim$0.5 cm range shown. A wider peak in delay space creates a narrower instrument response in wavenumber space, and makes it easier to know what feature in wavenumber space is being detected. This is shown by Figure 4, which is an effective measurement of the spectral shape using this limited-delay EDI technique. It is calculated by using the red curve of Figure 3 bottom as a filtering function. That is, taking the Fourier transform of the spectrum, multiplying by the red curve, then inverse Fourier transforming back to wavenumber space. A similar filtering using the classical R=3850 Gaussian response produces the gray curve. These show similar amplitude of the wiggles which correspond to the feature. The green curve is the native low resolution (R=70) spectrograph used alone, which cannot resolve the feature.

On the other hand, using multiple delays increases the readout noise, so there is some tradeoff to be considered. Reference 5 discusses readout noise in EDI measurements.

Moiré intensity fluctuations can be measured by dithering the delay, which is typically actuated by a voltage of a PZT transducer on which an interferometer mirror is mounted. At minimum, two 180 degree phase steps (exposures) allows determination of the nonfringing component, which is the ordinary spectrum. This is then subtracted from the original signal to reveal the fringing component, whose magnitude is proportional to the feature amplitude.

However, its better to use three 120 degree exposures, even though it incurs an additional readout noise, because it allows determination of the full complex shape of fringing component This yields both feature amplitude and determines the wavelength position (Doppler velocity).

3.1 Demonstration of EDI measurement of CO_2 feature

An EDI at the 5-m Hale telescope[2,5,10] has demonstrated measurement of this CO_2 feature in the telluric spectrum of starlight, with the spectrum shown in Figure 5. In comparison to the proposed IFS application, this measurement used a native spectrograph of much higher resolution (2700 instead of 70), and delays covering a range from zero to a high value, rather than a limited delay range. Its significant is that it shows that the phase stepped measurement technique and related software for processing it into spectra are operational in an observatory environment.

4. DISCUSSION

This effective EDI resolution boost, 70 to 4000, is especially important for Integral Field Spectrographs (IFS) which are often pixel limited (Fig. 1). We use the Gemini Planet Imager IFS resolution as a concrete example, even though it may lack the aperture to collect the needed photons from small exoplanets. The method can be generally applied to any spectrograph, but is especially useful for those that are pixel or otherwise resolution limited.

The EDI is also robust to other types of instrumental error which can often dominate photon noise. For example, EDI is naturally insensitive to fixed pattern noise that does not change synchronously to the applied phase dithering. The EDI is also resistant to the effects of wavelength drifts in the native disperser, since both the interferometer comb and the stellar spectrum drift the same amount and polarity, and thereby tend to cancel this error.

Since only 6 mm scale delays are needed, monolithic interferometer designs could be used which have an outside size of only a few cm. An example is a compact monolithic prism interferometer shown in Figure 6 constructed by the National Solar Observatory for Doppler velocimetry of sunlight. In principle this entire interferometer can be inserted into beam like a filter.

ACKNOWLEDGMENTS

This material is based upon work supported by the National Science Foundation under Grant No. AST-0505366, AST-096064, PAARE AST-1059158, NASA Grant NNX09AB38G, and under the auspices of the U.S. Department of Energy by Lawrence Livermore National Laboratory under Contract DE-AC52-07NA27344.

REFERENCES

[1] Macintosh, B. A., Graham, J. R., Palmer, D. W., Doyon, R., Dunn, J., Gavel, D. T., Larkin, J., Oppenheimer, B., Saddlemyer, L., Sivaramakrishnan, A., Wallace, J. K., Bauman, B., Erickson, D. A., Marois, C., Poyneer, L. A., and Soummer, R., "The Gemini Planet Imager: from science to design to construction," in [*Adaptive Optics Systems*], *Proc. SPIE* **7015**, 701518 (July 2008).

[2] Erskine, D. J., Edelstein, J., Wishnow, E. H., Sirk, M., Muirhead, P. S., Muterspaugh, M. W., Lloyd, J. P., Ishikawa, Y., McDonald, E. A., Shourt, W. V., and Vanderburg, A. M., "High-resolution broadband spectroscopy using externally dispersed interferometry at the Hale telescope: part 1, data analysis and results," *Journal of Astronomical Telescopes, Instruments, and Systems* **2**, 025004 (Apr. 2016).

[3] Erskine, D. J., Edelstein, J., Feuerstein, W. M., and Welsh, B., "High-Resolution Broadband Spectroscopy Using an Externally Dispersed Interferometer," *ApJ* **592**, L103–L106 (Aug. 2003).

[4] Erskine, D. J. and Edelstein, J., "Interferometric resolution boosting for spectrographs," in [*Ground-based Instrumentation for Astronomy*], Moorwood, A. and Iye, M., eds., *Proc. SPIE* **5492**, 190–199 (2004).

[5] Erskine, D. J., Edelstein, J., Wishnow, E., Sirk, M., Muirhead, P. S., Muterspaugh, M. W., and Lloyd, J. P., "High-resolution broadband spectroscopy using externally dispersed interferometry at the Hale telescope: part 2, photon noise theory," *Journal of Astronomical Telescopes, Instruments, and Systems* **2**, 045001 (Oct. 2016).

[6] Erskine, D. J., "Dispersed interferometers," in [*The WSPC Handbook of Astronomical Instrumentation*], Burrows, D. N. and Moore, A. M., eds., **Vol. 3**, World Scientific Publishing Company, Singapore (2019).

[7] Erskine, D. J. and Ge, J., "Novel Interferometer Spectrometer for Sensitive Stellar Radial Velocimetry," in [*Imaging the Universe in Three Dimensions: Astrphys. Advncd. Multi-Wavel. Imaging Devices*], van Breugel, W. and Bland-Hawthorn, J., eds., *ASP Conf. Series* **195**, 501–507 (2000).

[8] Erskine, D. J., "An Externally Dispersed Interferometer Prototype for Sensitive Radial Velocimetry: Theory and Demonstration on Sunlight," *PASP* **115**, 255–269 (Feb. 2003).

[9] van Eyken, J. C., Ge, J., and Mahadevan, S., "Theory of Dispersed Fixed-delay Interferometry for Radial Velocity Exoplanet Searches," *ApJS* **189**, 156–180 (2010).

[10] Muirhead, P. S., Edelstein, J., Erskine, D. J., Wright, J. T., Muterspaugh, M. W., Covey, K. R., Wishnow, E. H., Hamren, K., Andelson, P., Kimber, D., Mercer, T., Halverson, S. P., Vanderburg, A., Mondo, D., Czeszumska, A., and Lloyd, J. P., "Precise Stellar Radial Velocities of an M Dwarf with a Michelson Interferometer and a Medium-Resolution Near-Infrared Spectrograph," *PASP* **123**, 709 (June 2011).

[11] Ge, J., van Eyken, J., Mahadevan, S., DeWitt, C., Kane, S. R., Cohen, R., Vanden Heuvel, A., Fleming, S. W., Guo, P., Henry, G. W., Schneider, D. P., Ramsey, L. W., Wittenmyer, R. A., Endl, M., Cochran, W. D., Ford, E. B., Martín, E. L., Israelian, G., Valenti, J., and Montes, D., "The first extrasolar planet discovered with a new-generation high-throughput Doppler instrument," *ApJ* **648**, 683–695 (2006).